Journal of Instrumentation

PAPER • OPEN ACCESS

Study and development of diagnostic systems to characterise the extraction region in SPIDER

To cite this article: B. Segalini *et al* 2024 *JINST* **19** C01013

Jinst

Published by IOP Publishing for Sissa Medialab

Received: *August 11, 2023*
Revised: *November 7, 2023*
Accepted: *November 8, 2023*
Published: *January 15, 2024*

8th International Symposium on Negative Ions, Beams and Sources
Orto Botanico, Padova, Italy
2–7 October 2022

2024 JINST 19 C01013

Study and development of diagnostic systems to characterise the extraction region in SPIDER

B. Segalini,[a,b,*] **V. Candeloro,**[a,b] **C. Poggi,**[a] **G. Berton,**[a] **D. Fasolo,**[a] **L. Franchin,**[a] **B. Laterza,**[a] **M. Magagna,**[a] **L. Trevisan,**[a] **R. Pasqualotto,**[a,c] **G. Serianni,**[a,c] **M. Tollin**[a] **and E. Sartori**[a,b]

[a] *Consorzio RFX (CNR, ENEA, INFN, UNIPD, Acciaierie Venete SpA), Corso Stati Uniti 4, 35127 Padova, Italy*
[b] *Università degli Studi di Padova, Via VIII Febbraio 2, 35122 Padova, Italy*
[c] *ISTP-CNR, Institute for Plasma Science and Technology, Corso Stati Uniti 4, 35127 Padova, Italy*

E-mail: beatrice.segalini@igi.cnr.it

Abstract: SPIDER, an RF-driven negative ion source in the Neutral Beam Test Facility (NBTF), serves as the prototype for ITER's neutral beam injector (NBI). It is composed of 8 drivers powered by 4 RF generators, aiming to accelerate 50 A of negative hydrogen ions to 100 KeV with a beam uniformity target of 10%. The experiment, launched in 2018, tested negative ion production using caesium. Results match those of similar facilities, but SPIDER faces challenges due to its size, multiple drivers, and non-uniform plasma expansion. These issues impact beam uniformity, preventing the machine from reaching expected performance. To address this, SPIDER initiated a significant shutdown at the end of 2021 for improvements.

One the most important aspects studied during the first experimental campaign is source uniformity, addressed both in terms of plasma and of caesium distribution. The latter is particularly relevant since its quality is directly related to the beam uniformity and divergence. To have more insight about these issues, monitoring the plasma properties in the extraction region is crucial, hence in the present contribution, the design and development of two new diagnostic systems are described: a movable Langmuir probe and a Retarding Field Energy Analyser (RFEA).

The first can provide a vertical scan of the main plasma parameters close to the plasma grid. The spatial resolution would improve with respect to the already installed set of fixed Langmuir

*Corresponding author.

https://doi.org/10.1088/1748-0221/19/01/C01013

probes embedded in the grid system, and the newly installed diagnostic could interact with other sensors to produce complementary measurements (namely, electron photo-detachment). The latter, instead, allows the monitoring of the positive ion energy distribution: positive ions, in fact, can be precursors of the negative ones produced at the caesiated surface, but also influence the energy of negative ion and their extraction probability and thus collecting information about their energy distribution allows inferring details about the extracted negative ion beam.

The two diagnostics are designed focusing on the experimental constraint of integrating the diagnostics in a harsh and complex environment such as SPIDER plasma: a preliminary study of the placement inside the source is carried out, then the electrode of the movable probe and the RFEA sensor are sized according to the spatial and energy resolution requested by the system.

KEYWORDS: Plasma diagnostics - probes; Ion sources (positive ions, negative ions, electron cyclotron resonance (ECR), electron beam (EBIS))

2024 JINST 19 C01013

Contents

2024 JINST 19 C01013

1 Introduction: diagnostics in NBI negative ion sources

One of the main elements of heating systems for thermonuclear plasmas, based on neutral beam injection, is the (negative) ion source. In fact, the source itself determines several extracted beam parameters, including intensity, shape, emittance, and operation mode (continuous or pulsed). Because of this, it is crucial to characterise the source operation and enhance its performances in order to meet the ITER NBI standards. With this aim, many test facilities are built around the world, and in all of them diagnostic systems are installed for investigating the source plasma properties and beam production.

Two very important experiments are located in Garching (Germany), at the Max Plank Institute for Plasma Physics (IPP): BATMAN (BAvarian Test MAchine for Negative ions) and ELISE (Extraction from a Large Ion Source Experiment). Both are RF-driven negative ion sources, equipped with a 3 or 4 grid systems and with a comprehensive system of diagnostics, thought to be respectively $1/8$ and $1/2$ of ITER full size negative ion source.

On BATMAN, which was recently upgraded with a new grid system and with new permanent magnets embedded in the grids ([1, 2]), and hence re-named BUG-MLE (BATMAN UpGrade with Mitica Like Extraction), the beam optics can be studied with three main diagnostics. Beam Emission Spectroscopy (BES) can be performed with vertical resolution at two separate axial positions and provides information on the characteristics of both the single beamlet or a group of beamlets, depending on the grid masking [3]. A Carbon Fibre Composite (CFC) tile calorimeter is also present on BUG-MLE, built taking as inspiration [4]. It is a retractable tile which, thanks to an infrared camera, can collect beamlet thermal footprints and hence be used to examine the characteristics of single beamlets [5]. Finally, at the end of the beam path, a Copper Wire (CW) calorimeter [6] can be found. This instrument can provide information also about beam power density, although its resolution is rougher with respect to the CFC. ELISE has a similar set of diagnostic instruments. A calorimeter equipped with thermocouples is present, together with some water calorimetry tools

and IR cameras for imaging, in addition to 20 lines of sight of BES [7]. This very complete set of diagnostics allows a thorough understanding of beam uniformity and the measurement of the overall beam divergence, even though single beamlets are not resolved.

Other important test facilities for ITER are located in Japan [8]. In particular, the National Institutes for Quantum and Radiological Science and Technology (QST) in Naka, Japan, hosts a massive negative ion source producing high power negative ion beams, with energy of 500 keV, current of 22 A (130 A m^{-2} in the current density) and beam-on time of 100 s [9]. A large negative ion source with a 1.2 m long arc discharge chamber and a multi-aperture three-stage accelerator have been built to reach the goal values. Also in this caesium (Cs) seeded source spectroscopy and calorimetry methods are employed to evaluate beam profiles and plasma parameters of the N-NBI source [10]. A comprehensive review can be found in [11, 12].

The largest test facility is hosted in Padua and is ITER full-scale negative ion beam source: SPIDER. This machine is fundamental in the development of ITER NBI heating system, and aims to investigate and optimise beam uniformity, negative ion current density, and beam optics at low energy. Doing so is not a trivial task, since non-uniformities arise due to the presence of a magnetic field and of borders/edges in the source plasma, and they are enhanced by the big size of the experiment. Single beamlet optics are determined by the perveance; in a multi-aperture system having different beamlet currents leads to a locally different divergence and accelerated current over the beam area. They can result in localised heat loads, and eventually lead to power losses along the accelerator and beamline, compromising plasma heating and potentially damaging the NBI components. In fact, during the 3 years-long campaign in which also caesium injection has been tested, the beam profile exhibited non-uniformities, particularly localised peaks, which were enhanced by increasing the magnetic filter field and extraction voltage [13].

Hence, assessing plasma profiles is crucial for improving source performances. To do so, SPIDER is provided with a set of spatially resolved source and beam diagnostics, installed to monitor different plasma parameters simultaneously [14]. Power and heat loads are measured via calorimetry and a set of surface thermocouples. A retractable Carbon fiber composite tile (STRIKE [4]) calorimeter is installed on the beam path so that it can collect beamlet footprints and estimate beamlet alignment and divergence. Several electrostatic probes are employed for deriving plasma electron temperature and density and to assess overall plasma uniformity. Spectroscopy is also utilised: Optical emission (OES), Cavity ring down (CRDS), Laser Absorption (LAS) and Beam Emission Spectroscopy (BES) are all utilised to derive a huge variety of plasma parameters, providing spatial profiles of densities (negative ions, electrons, caesium) and electron temperature. In addition, an Allison Emittance Scanner [15] and a set of tomography cameras [16] allow to measure vertical emittance of single beamlets and beam uniformity in 2D respectively.

1.1 Integrating the diagnostic system

Despite all the instruments already installed on SPIDER (described in [17]), the spatial resolution of the existing diagnostic systems in the SPIDER source is still not enough to investigate some inhomogeneities in beamlet profiles that were outlined during the experimental activities [14]. In fact, in both Cs-free operations and during caesium injection, the global imbalance of current density in the vertical direction corresponded to the non-uniform distribution of positive ions in the extraction region. Increasing the caesium injection rate resulted in higher positive and negative ion densities,

2024 JINST 19 C01013

leading to increased electronegativity and improved caesium distribution across the plasma grid. As a consequence, especially during caesiation, it is important to monitor the positive ion energy distribution, since positive ions are precursors of surface emitted negative ones: for this reason, the diagnostic system VICTOR is designed, including more specifically a Retarding Field Energy Analyser (section 2.1).

In addition, within beamlet groups, central beamlets had higher current density compared to those at the edges. This local non-uniformity could be attributed to vertical plasma expansion and the influence of the bias plate metal surface in the horizontal direction. Thus, analysing more in detail the plasma properties within one beamlet group is important to understand how to optimise negative ion extraction: with this aim, in the present paper the design of a vertical movable Langmuir probe with a finer spatial resolution is displayed in 3.

This upgrades however face some distinctive challenges and complexities. SPIDER's environment is characterised by the presence of high voltage differences and currents and of vacuum. Material compatibility with these conditions is one of the first requirements. Besides, the diagnostics design is demanded to be robust to thermo-mechanical stress given the possible insurgence of thermal gradients (and hence dilation) and to their poor maintainability. It is also essential to define a proper alignment procedure for the linear actuators, which need to cross areas with significant voltage differences and to be integrated in vacuum. Finally, the presence of RF disturbances also has to be taken into account.

2 VICTOR

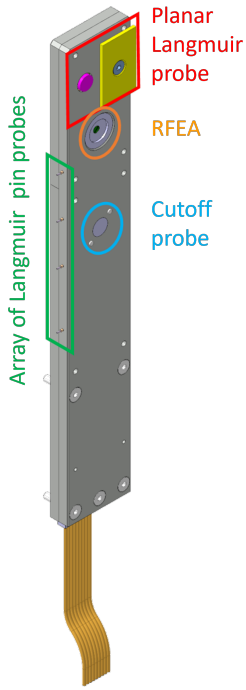

Figure 1. 3D CAD representation of VICTOR.

VICTOR (Very Interesting Complex Tool for Observing RF plasma) is a diagnostic system including several sensors as shown in figure 1. It is composed of:

- a Retarding Field Energy Analyzer (RFEA), described in sub-section 2.1 (orange circle);
- a planar Langmuir probe for measuring the plasma floating potential V_f (sub-section 2.2, red square);
- an array of Langmuir pin probes (also described in sub-section 2.2, green rectangle);
- a cut-off pin probe to measure the plasma frequency (sub-section 2.3, cyan circle).

2.1 Retarding Field Energy Anlayzer

The main diagnostic present on VICTOR is the RFEA: a sensor able to measure the (positive) ion energy distribution through a set of 4 polarised grids. RFEAs are well known in literature ([18, 19]) and have already been used in other fusion-related experiments (for example in [20, 21]).

2024 JINST 19 C01013

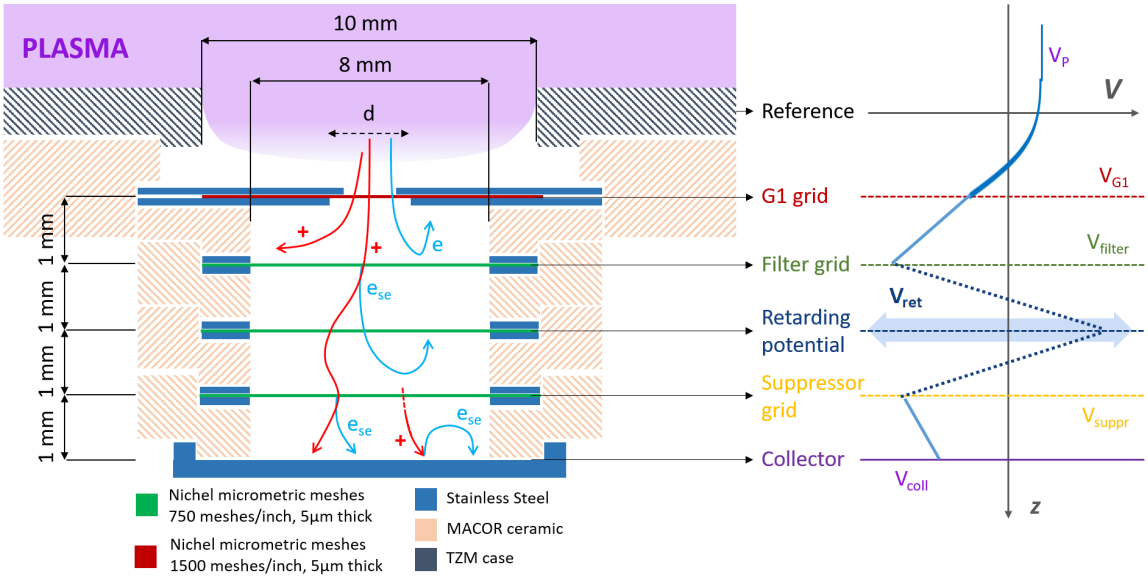

Figure 2. Functioning principle of a RFEA sensor. Left: section with grid distances, aperture diameters and materials used for manufacturing. Right: potentials involved during RFEA operation, starting from the plasma potential V_p, through the various grid bias potentials (V_{G1}, V_{filter}, V_{ret}, V_{suppr}), to the collected particles voltage V_{coll}. Axial direction in both schemes is labelled with z.

Their working principle is displayed in figure 2: the 4 grids, made of nickel micrometric meshes, act as particle selectors in order to filter them. The first grid (G1) is negatively polarised (≈ -30 V) with respect to the reference, in order to attract positive ions. If some fast electrons are by chance to enter the RFEA, the second grid (Filter) is also set a significantly negative voltage (≈ -100V) to repel the negatively charged particles. The following grid is the one actually allowing the measurement of ion energy to occur: in fact, it performs a voltage sweep, selecting particles only with a certain z-component of their velocity. The characteristic curve analysed will be depending on V_{ret}. Along their path in the grid system (which is a set of electrostatic lenses), it could happen that some electrons are produced by secondary emission phenomena at the surface. To reduce their contribution to the collected current, the last grid is also polarised at a negative voltage (generally the lowest involved, $\approx$ 120V), so that these particles are not collected. This last grid is called suppressor grid as it repels secondary electrons emitted from the collector. Of course, if the impact of ions on the suppressor grid itself is the cause of the birth of secondary-emitted electrons, they will be nevertheless present in the final energy distribution.

A similar sensor was already produced and tested at NIFS in a joint campaign with RFX [22]. The experimental conditions in SPIDER, however, are significantly different, given that SPIDER is a RF source and not an arc one, which reflect on the plasma parameter values and profiles. More specifically, at high plasma density, the space charge effect due to same-charge repulsion inside the RFEA, is more evident, leading to mixing axial and radial components of the ion velocities (i.e., loss of energy resolution) and in extreme cases to particle losses onto the sensor walls. One possible way to prevent this effect inside the sensor is to design the gaps between the grids as short as possible; on the other hand, a smaller gap implies a rougher energy resolution, as described in [23]. A trade-off

2024 JINST 19 C01013

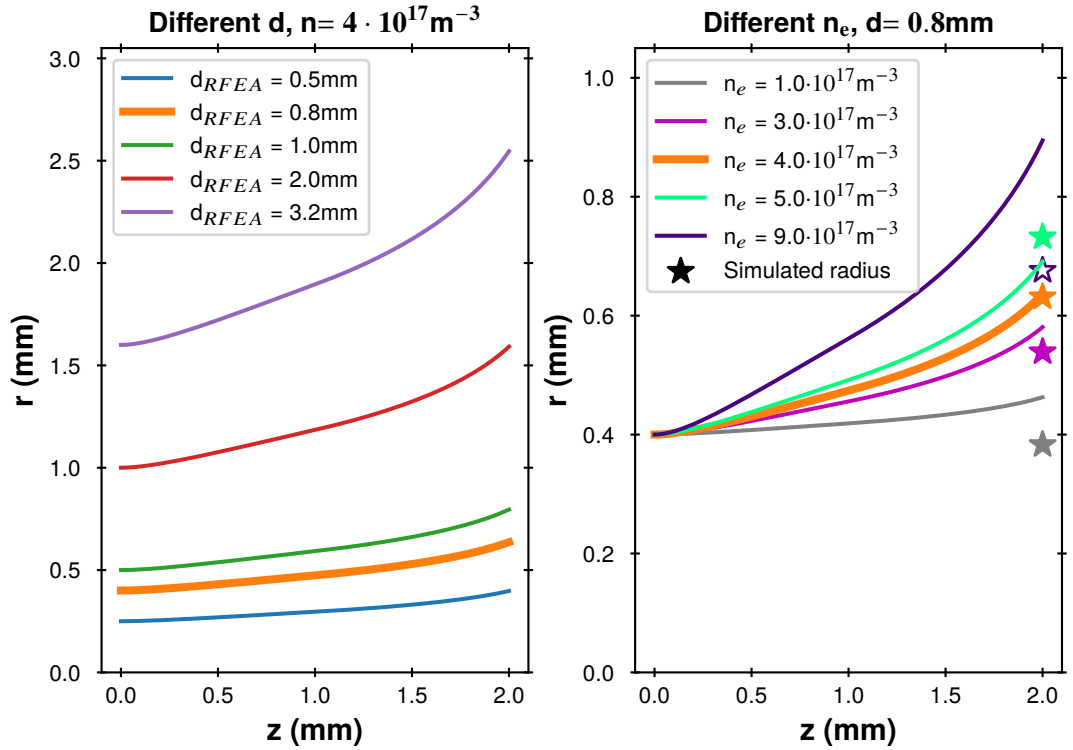

Figure 3. Left: particle envelope trajectories for different aperture diameters, for $n_e = 4 \cdot 10^{17}\mathrm{m}^{-3}$. Right: particle envelope trajectories for different plasma densities, for $d = 0.8$ mm, and their corresponding numerical comparison. Thickest orange line is the same data between left and right graph. Hollow star represents the non-matching point (simulation/theory).

is necessary between these opposite requirements on the grid gap. Another way to reduce the space charge repulsion for an identical transmitted current is to adopt a multi-aperture configuration for the front aperture (shown as d in figure 2). In fact, the growth of a charged beam envelope depends on its current rather than current density, as a consequence the same total current can be less influenced by this phenomenon if carried by multiple beamlets.

A first analytical computation can be derived by solving the differential equation (4) of [24], which gives an estimate of the envelope of an ion beam subject to space charge effects. Different orifice diameters and plasma densities were considered; particle envelopes from the front aperture to the retarding potential grid are represented in figure 3 with lines. Furthermore, to define the most suitable radius of the front aperture, a set of simulations was performed to derive the spread of the positive-ion beam after a gap of 1mm between two surfaces at different potentials (i.e. plasma-facing grid and filter potential grid), using a 3D test particle Monte Carlo code [25]. Two possible designs were considered: one with a single aperture on the plasma-facing grid, and one with multiple-apertures (3). The estimated radius at the retarding potential grid for the case $d = 0.8$mm with this method is reported for different plasma densities in the right part of figure 3 (stars).

Observing the left part of 3, it is clear that the larger the front diameter, the more evident the spread of the beam due to the space charge effects. Besides, this spread is worsened by the increasing density n_e, as it can be seen from the graph on the right. In the same picture, one can notice that

2024 JINST 19 C01013

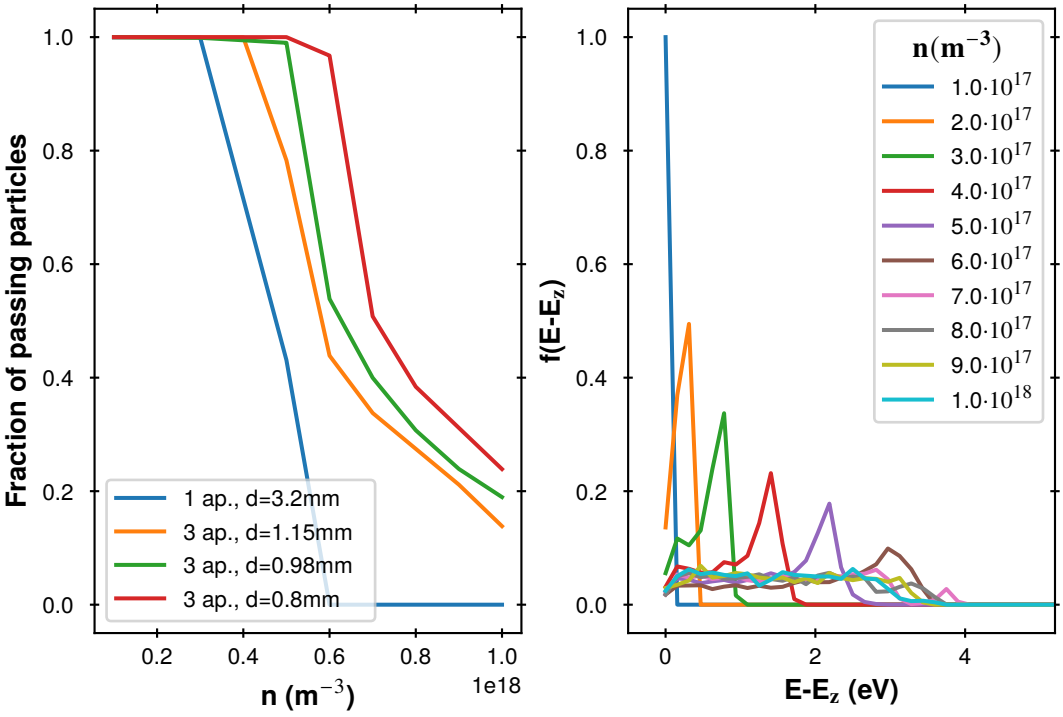

Figure 4. Left: fraction of tracked particles arriving at the retarding potential grid as a function of the plasma density, for different aperture diameters and configurations. Right: non-axial energy distribution at the retarding grid for different plasma densities, which is an estimation of the sensor energy resolution.

agreement between the numerical simulations and the analytical solutions is good, namely the ending point of the envelope trajectory is very close to the corresponding simulated radius. However, this agreement is valid only for the lower plasma densities, due to the loss of particles on the sensor walls when the space charge effects become too significant: it is the case of $n_e = 9 \cdot 10^{17}\mathrm{m}^{-3}$ (and its corresponding hollow star).

Figure 4 on the left shows the percentage of simulated particles that actually arrive at the retarding potential grid: it can be seen, in fact, that for the bigger diameter ($d = 3.2\,\mathrm{mm}$) half of the starting particles are already lost for densities of $5 \cdot 10^{17}\mathrm{m}^{-3}$. The fraction of passing particles significantly improves for smaller aperture diameters. Higher densities, however, induce an effect on the energy distribution: as it can be seen looking at the right graph in figure 4, the non-axial energy distribution shows a peak that moves towards higher energies with increasing n. This means that a broadening of the beam is nevertheless expected, with an induced broadening of the final energy distribution of about 2eV for the expected electron density close to the extraction region (a few $10^{17}\mathrm{m}^{-3}$).

So in conclusion, the final design for the front mesh of the RFEA sensor installed on VICTOR will consist of 7 apertures of 0.8mm diameter, after evaluating the improvement between single and 4-aperture designs.

2024 JINST 19 C01013

2.2 Langmuir probes

Langmuir probes complete the set of diagnostics included in VICTOR. The most important one is the one in the red box of figure 1: it is a fixed planar probe with a molybdenum compensation electrode, with the same design described in [26]. The flat probe allows the measurements of the floating potential V_f, required to protect the fragile grids from the plasma: in fact, it is important to keep the front grid G1 at a lower potential with respect to V_f, because otherwise a big number of electrons would be attracted, heating significantly the grid, in addition to providing a biased energy distribution at the end of the sensor. Besides, the sensor could be used as a further reference to the already existing set of fixed probes installed on the BP, concerning their RF compensation.

In addition to this large probe, a set of 4 pin probes (green box in figure 1) is present on the side of VICTOR. These sensors, polarised to be in the ion saturation branch of the I-V characteristic curve, are used to provide an estimate of the plasma density in correspondence of the last 3 beamlet rows in the beamlet group, while the fourth one could give an idea of how the plasma behaves just outside the extraction area. Their measurements will help in characterising locally the plasma with a space resolution which was not present on SPIDER before. They will be composed by a 8 mm long tungsten wire with diameter of 0.5 mm, isolated through an alumina thin tube and ceramic glue.

2.3 Cut-off probe

The fraction of the different plasma species (negative and positive ions and electrons) in the expansion region of a caesiated negative ion source can greatly vary with the machine parameters, and this variation strongly affects the uncertainty on the estimation of the densities of the species. To this purpose, a cut-off probe [27] is also included in VICTOR design, placed in the light blue circle in figure 1. It is composed of two tungsten electrodes 5 mm length and 0.5 mm thickness, placed at a distance of 3 mm and screened from the plasma with two alumina tubes of 0.2 mm wall thickness. The two pins are connected to the two ports of a network analyser, from the acquired spectra it is possible to directly measure the plasma frequency $f_p = \omega_p/2\pi$ in order to infer the electron density following the relation:

$$\omega_p = \sqrt{\frac{n_e e^2}{\epsilon_0 m_e}} \tag{2.1}$$

with n_e the density of the plasma electrons, e the electron charge, m_e the electron mass and ϵ_0 the permittivity of free space. For an electron density between 1×10^{15} m^{-3} and 5×10^{17} m^{-3} the corresponding plasma electron frequency is between 280 MHz and 6.3 GHz.

3 Movable Langmuir probes

Thanks to the installation of a PG mask [28], beam diagnostics were able to detect vertical non-uniformities in the SPIDER beam profile within the beamlet group scale [29]. The influence of the mask itself on these results was ruled out [30], supporting the possible correlation with the source properties in the extraction region. Although this region is already characterised by a matrix of electrostatic sensors embedded on both the Plasma Grid (PG) and Bias Plate (BP) apertures, the spatial distribution of these sensors is not optimal for accurately measuring the vertical profiles of plasma properties. In order to improve the overall spatial resolution of source diagnostics in

2024 JINST 19 C01013

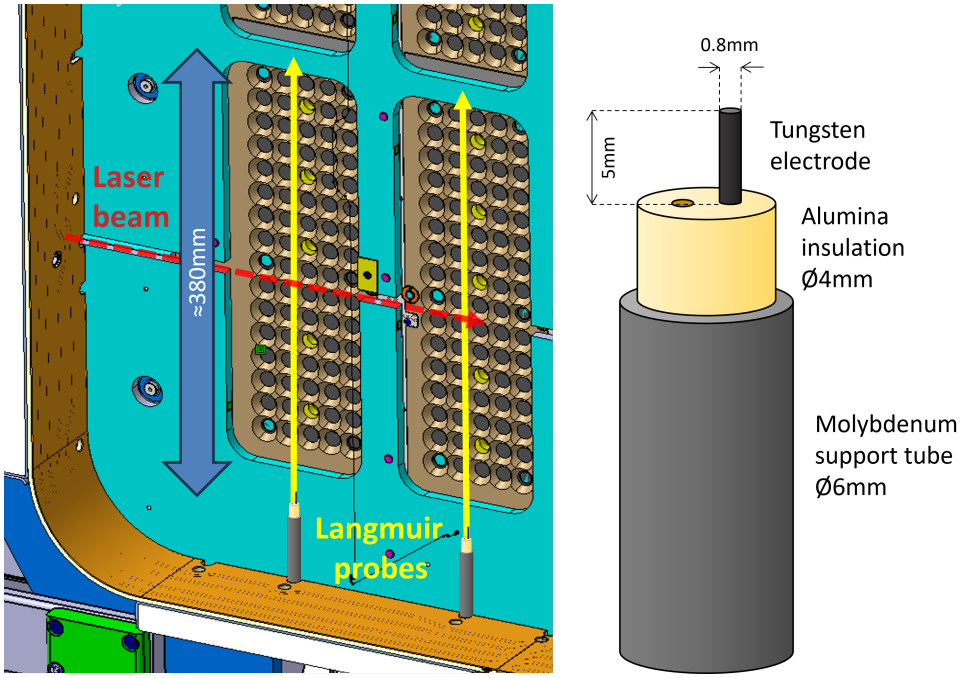

Figure 5. Left: schematics of movable probe system inside SPIDER. The picture shows the inside of the expansion region, the bias plate (cyan) and the plasma grid (beige). The path covered by the movable probe is represented in yellow, and the total stroke is highlighted with the blue arrow. The red dashed arrow shows the view-port for the Nd:YAG laser that could be used for the electron photo-detachment. Right: representation of the probe tip. Please note that the vertical accuracy is limited to the vertical extension of the electrode.

the extraction region, two vertical movable probes (VERAs, Vertical Extraction Region Analysers) will be installed in SPIDER. These probes will sample the plasma properties at a distance of roughly 10 mm from the BP surface, helping to correlate the source plasma behaviour with the beam properties.

As shown in figure 5, the probes enter the expansion chamber from its bottom surface, and travel parallel to the grids with a total stroke of 380 mm, which is sufficient to cover entirely the bottom beamlet group. To this purpose, two independent linear actuators will be installed in front of the two inner beamlet groups: this configuration will also allow to investigate asymmetries along the horizontal direction, already detected during the previous experimental campaigns [13]. Besides mechanical stability constraints, the maximum travel distance of the probes is limited by the available space at the bottom of the source; in fact, the entire system needs to fit within the volume defined by the electrostatic shield of the source.

The probe shaft is composed of a multi-bore alumina tube (Al_2O_3) of 4 mm diameter, shielded by a molybdenum tube of 0.75 mm thickness. The metallic shielding was introduced to protect the alumina tube from back-streaming positive ions coming from the accelerator. With the probe shaft being metallic on the outside, the alignment system is designed in such a way that the probes will not be in electrical contact with both the lateral walls and the BP at the same time, as the latter have different electrostatic potentials. To this purpose, a PEEK insulating socket has been designed to prevent electrical contacts.

2024 JINST 19 C01013

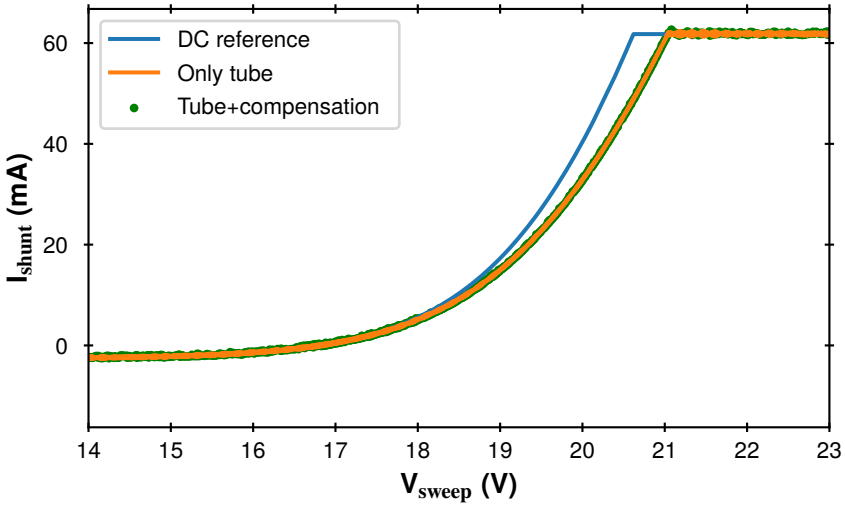

Figure 6. Results of LTSpice simulations: comparison between I-V curves of the two possible compensation configurations and a DC reference curve.

Concerning the probe head design, several solutions can be applied according to experimental objectives of SPIDER operation. As a first step, the probes will be operated as single Langmuir probes with the aim of measuring electron density and temperature profiles at the bottom segment, where they are expected to be larger due to drifts motions inside the expansion chamber [14]. To do so, the probes will be operated in sweeping mode, measuring the entire current-voltage (CV) characteristic. As the magnetic filter field is expected to lower the electron temperatures down to a few eV, it will be necessary to design a proper RF compensation for the electrodes. More precisely, two possible options for passive compensation were considered in the design phase: one including a compensation electrode in the design consisting of a thin Tungsten wire wrapped on the exposing part of the alumina insulating tube, with an equivalent area of $\approx 70\text{mm}^2$, the other configuration considers not compensating the main electrode but exploiting the molybdenum tube instead: in fact, the capacitance of the metallic tube moving in front of a polarised plate could have a sufficient compensating effect. Besides, a choke filter composed of one inductance and one capacity in parallel will be used to actively compensate the signal. The filter components will be tuned to maximise the filter impedance at the RF frequency of the drivers, which is expected to be 1 MHz within 10% range, and higher harmonics, similarly to the ones already installed in SPIDER on the set of horizontally movable Langmuir probes [31].

Some LTSpice simulations were performed to determine the best design, and their results are reported in figure 6. As it can be noticed, the effect on the I-V curve of the large capacitance induced by the moving tube in front of the BP makes redundant the addition of an additional compensation electrode.

Another type of probe head is under design in view of the application of the laser photo-detachment technique [32] in SPIDER: this requires the probe to be aligned with a Nd:YAG laser for measuring the negative ion density. In this case, the probe electrode dimensions will be defined taking into account the laser cone section (the probe electrode radius shall be smaller than the laser cone radius). The laser will deliver enough power to neutralise the negative ions along its line of sight: in

2024 JINST 19 C01013

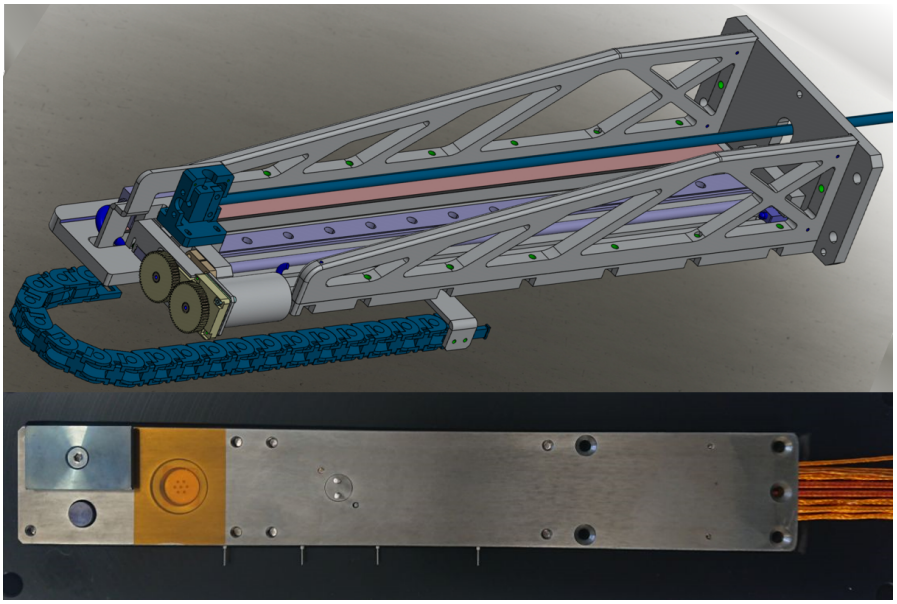

Figure 7. Top: linear actuator CAD drawing for VERA, designed specifically to fit the tight space below SPIDER's extraction region and to fulfil the alignment requirements. Bottom: manufactured version of VICTOR, with Kapton tape protecting the 7-apertures first grid of the RFEA, ready to be installed on SPIDER.

order to collect the detached electrons, the probe head will be positively polarised with respect to the plasma potential. The influence of the magnetic filter field on the measurement shall also be analysed.

4 Conclusions and future work

With the objective of comprehending and optimising negative ion extraction, it is essential to thoroughly investigate the ion source using spatially resolved diagnostic systems, particularly in the region abundant in negative ions. The presence of spatial variations on the scale of beamlet groups underscores the necessity for enhanced diagnostics to improve overall beam uniformity. As the overall non-uniformity can be attributed to plasma generation, expansion, or both, the inclusion of permanent and movable measuring systems is imperative to study the real-time effect of source control parameters. This is particularly relevant in multi-driver giant sources that are prone to spatial variations in beam parameters, like SPIDER.

The already comprehensive set of source diagnostic systems is going to be improved also thanks to the addition of the diagnostics described in this paper. The two movable Langmuir probes will provide a better spatial resolution for estimating plasma parameters, allowing to outline plasma asymmetries close to the extraction area. VICTOR, in addition to other Langmuir probes, will provide a measurement of the positive ion energy distribution, via the RFEA whose design has been described in this manuscript; besides, the cut-off probe will complete the set of measurements by attempting to estimate the plasma frequency.

VICTOR and the movable Langmuir probe systems are now under manufacturing (see figure 7), and will be installed on SPIDER soon: in the near future, testing of the sensors is anticipated in preparation for the upcoming experimental campaign.

2024 JINST 19 C01013

Acknowledgments

This work has been carried out within the framework of the EUROfusion Consortium, funded by the European Union via the Euratom Research and Training Programme (Grant Agreement No 101052200 — EUROfusion). Views and opinions expressed are however those of the author(s) only and do not necessarily reflect those of the European Union or the European Commission. Neither the European Union nor the European Commission can be held responsible for them.

This work has been carried out within the framework of the ITER-RFX Neutral Beam Testing Facility (NBTF) Agreement and has received funding from the ITER Organization. The views and opinions expressed herein do not necessarily reflect those of the ITER Organization.

References

[1] B. Heinemann et al., *Upgrade of the batman test facility for h- source development*, *AIP Conf. Proc.* **1655** (2015) 060003.

[2] C. Wimmer et al., *Overview of recent and upcoming activities at the batman upgrade test facility*, *J. Phys. Conf. Ser.* **2244** (2022) 012051.

[3] U. Fantz et al., *Advanced nbi beam characterization capabilities at the recently improved test facility batman upgrade*, *Fusion Eng. Des.* **146** (2019) 212.

[4] A. Rizzolo et al., *Final design of the diagnostic calorimeter for the negative ion source spider*, *Fusion Eng. Des.* **123** (2017) 768.

[5] G. Orozco et al., *Design and first results of a retractable 1D-CFC beam target for BATMAN upgrade*, *Fusion Eng. Des.* **165** (2021) 112225.

[6] R. Nocentini, F. Bonomo, B. Heinemann, A. Hurlbatt and I. Mario, *Long-pulse diagnostic calorimeter for the negative ion source testbed batman upgrade*, *Rev. Sci. Instrum.* **92** (2021) 023504.

[7] D. Wünderlich et al., *Progress of the elise test facility: towards one hour pulses in hydrogen*, *Nucl. Fusion* **56** (2016) 106004.

[8] JT-60SA, https://www.jt60sa.org/wp/.

[9] M. Kashiwagi et al., *100 s negative ion accelerations for the JT-60SA negative-ion-based neutral beam injector*, *Nucl. Fusion* **62** (2022) 026025.

[10] M. Ichikawa et al., *Achievement of stable negative ion production with cs-seeded for long pulse beam operation in the prototype of cs-seeded negative ion source for jt-60sa*, *Rev. Sci. Instrum.* **91** (2020) 023502.

[11] K. Tsumori and M. Wada, *Diagnostics tools and methods for negative ion source plasmas, a review*, *New J. Phys.* **19** (2017) 045002.

[12] K. Tsumori and M. Wada, *A review of diagnostic techniques for high-intensity negative ion sources*, *Appl. Phys. Rev.* **8** (2021) 021314.

[13] G. Serianni et al., *Spider, the negative ion source prototype for iter: Overview of operations and cesium injection*, *IEEE Trans. Plasma Sci.* **51** (2023) 927.

[14] G. Serianni et al., *Spatially resolved diagnostics for optimization of large ion beam sources*, *Rev. Sci. Instrum.* **93** (2022) 081101.

2024 JINST 19 C01013

[15] C. Poggi et al., *Design and development of an Allison type emittance scanner for the SPIDER ion source*, *Rev. Sci. Instrum.* **91** (2020) 013328.

[16] M. Ugoletti, M. Agostini, A. Pimazzoni, E. Sartori and G. Serianni, *Spider beam homogeneity characterization through visible cameras*, *IEEE Trans. Plasma Sci.* **50** (2022) 3913.

[17] R. Pasqualotto et al., *Improvement of spider diagnostic systems*, *Fusion Eng. Des.* **194** (2023) 113889.

[18] I.H. Hutchinson, *Principles of Plasma Diagnostics*, 2nd edition, Cambridge University Press (2002) [DOI:10.1017/CBO9780511613630].

[19] J.A. Simpson, *Design of retarding field energy analyzers*, *Rev. Sci. Instrum.* **32** (1961) 1283.

[20] C. Ullmann et al., *Investigation of ion beam space charge compensation with a 4-grid analyzer*, *Rev. Sci. Instrum.* **87** (2016) 02B938.

[21] R.A. Pitts et al., *Retarding field energy analyzer for the jet plasma boundary*, *Rev. Sci. Instrum.* **74** (2003) 4644.

[22] C. Poggi, *Numerical and experimental study of the physics of negative ion beams*, Ph.D. Thesis, Ghent University (2021).

[23] Y. Sakai and I. Katsumata, *An energy resolution formula of a three plane grids retarding field energy analyzer*, *Jap. J. Appl. Phys.* **24** (1985) 337.

[24] G. Serianni et al., *Neutralisation and transport of negative ion beams: physics and diagnostics*, *New J. Phys.* **19** (2017) 045003.

[25] B. Segalini, C. Poggi, M. Fadone, G. Serianni and E. Sartori, *Study of positive ion transport to the plasma electrode in giant rf negative ion sources*, *Fusion Eng. Des.* **194** (2023) 113736.

[26] M. Spolaore, G. Serianni, A. Leorato and F.D. Agostini, *Design of a system of electrostatic probes for the rf negative ion source of the spider experiment*, *J. Phys. D* **43** (2010) 124018.

[27] K. You et al., *A cutoff probe for the measurement of high density plasma*, *Thin Solid Films* **547** (2013) 250.

[28] M. Pavei et al., *Spider plasma grid masking for reducing gas conductance and pressure in the vacuum vessel*, *Fusion Eng. Des.* **161** (2020) 112036.

[29] A. Pimazzoni et al., *Co-extracted electrons and beam inhomogeneity in the large negative ion source spider*, *Fusion Eng. Des.* **168** (2021) 112440.

[30] E. Sartori, V. Candeloro, M. Fadone, A. Pimazzoni and G. Serianni, *Influence of plasma grid-masking on the results of early spider operation*, *Fusion Eng. Des.* **194** (2023) 113730.

[31] E. Sartori et al., *Development of a set of movable electrostatic probes to characterize the plasma in the iter neutral beam negative-ion source prototype*, *Fusion Eng. Des.* **169** (2021) 112424.

[32] M. Bacal, *Photodetachment diagnostic techniques for measuring negative ion densities and temperatures in plasmas*, *Rev. Sci. Instrum.* **71** (2000) 3981.

2024 JINST 19 C01013